

Figure 2. Field-ionization mass spectrum (FIMS) of the mixture of methylated fullerenes.

contains a single resonance at $\delta(^{13}\text{C})$ 156.7 for the reduced C_{60} . This *deshielding* of 14 ppm/carbon atom is remarkable, because generally carbanion carbons are *shielded* compared to their neutral precursors. Such deshielding in the case of C_{60} polyanion may be rationalized by populating the antibonding LUMO.¹⁴ The ^{13}C NMR spectrum which indicates the presence of reduced C_{70} was obtained at -80°C to improve the signal to noise ratio (see Figure 1b). The five resonances are at 158.3, 152.3, 149.6, 137.9, and 133.7 ppm in a 1:2:1:2:1 ratio, respectively, showing a slight overall deshielding compared to neutral C_{70} .¹⁵ We also reduced chromatographically purified (alumina and hexanes/toluene as eluant) samples of C_{60} to confirm our results. Further, we obtained a ^7Li spectrum of the reduced $\text{C}_{60}/\text{C}_{70}$ solution at -80°C which showed a fairly sharp resonance at +1.6 ppm (versus 1 M LiCl in THF). The ^7Li spectrum at room temperature was extremely broad, indicating a solvent-separated ion pair/contact-ion pair equilibrium in the temperature range studied.¹⁶

The polyanions generated contain an even number of electrons, judging from the sharp ^{13}C NMR signals, indicating a diamagnetic species.¹⁷ Since a previous cyclic voltammetry study^{10a} (vide supra) indicates reversible three-electron reduction for each fullerene, it seems likely under the present conditions that C_{60} and C_{70} each accepted four or more electrons. Theoretical calculations^{4a,b,d-z,m} indicate a triply degenerate LUMO for C_{60} , making it possible that a hexaanion of C_{60} could have been generated. A similar situation exists for C_{70} , in which the LUMO and doubly degenerate LUMO¹⁺ are closely spaced.^{4d} Attempts to determine the exact number of electrons added to fullerenes **1** and **2** by quenching the polyanions with D_2O were unsuccessful. The isolated product mixture when analyzed by field-ionization mass spectrometry (FIMS) displayed only a mixture of C_{60} and C_{70} . Presumably, the deuterated product mixture undergoes rapid oxidation to regenerate the more stable starting fullerenes in both cases.¹⁸

Alkylation of the C_{60} and C_{70} polyanion mixture with excess methyl iodide, on the other hand, yielded a light brown solid that FIMS (Figure 2) indicates to be a mixture of polymethylated fullerenes (also confirmed by ^1H and ^{13}C NMR, $\delta(^1\text{H}) \approx 0.06$, $\delta(^{13}\text{C}) \approx 1.0$). The FIMS analysis show a range of methylated

products from one all the way to 24 methyls. There is a preponderance of products with even numbers of methyl groups (with six and eight predominating). The nominal masses of the products with odd numbers of methyl groups correspond to the addition of a methyl group(s) and a hydrogen atom(s). However, the exact mechanism of the observed alkylation is not yet clear but possibly involves electron transfer to methylated fullerenes during quenching. This result represents the first functionalization of C_{60} and C_{70} via alkylative C-C bond formation. We will report complete characterization (NMR, IR, X-ray diffraction) of the methylated products. The achieved methylation of C_{60} and C_{70} fullerenes opens up the possibility of other functionalizations with alkyl halides, as well as other versatile substituents such as trialkylhalosilanes. Direct Barbier type reactions were successfully carried out in the case of chlorotrimethylsilane. We are continuing our studies toward diverse functionalization of fullerenes.

We also carried out oxidation studies on C_{60} and C_{70} using SbF_5 in SO_2ClF solution, a system found highly efficient for the oxidation of polycyclic aromatics to their dications.¹⁹ Green-colored solutions were obtained that gave extremely broad ^{13}C NMR spectra at all temperatures employed (-80°C to room temperature). Similar spectra were obtained by using SbF_5 and Cl_2 as the oxidant in SO_2ClF solution. It appears that radical cations have been generated and no diamagnetic di- or polycations were formed. This is not surprising since electrochemical studies⁹ and FT-ICR experiments²⁰ indicate a high oxidation potential for C_{60} .

Acknowledgment. Support of the work at USC by the National Science Foundation, the National Institutes of Health, and the Office of Naval Research is gratefully acknowledged. The work at SRI International was supported by the IR & D fund. We thank Professor F. Wudl for a sample of pure C_{70} and together with Professor F. Diederich for a preprint of their work describing the details of the chromatographic separation and cyclic voltammetry of the fullerenes. We also thank Dr. Frank Devlin for carrying out ESR studies.

(19) Olah, G. A.; Forsyth, D. A. *J. Am. Chem. Soc.* **1976**, *98*, 4086.

(20) Zimmerman, J.; Eylur, J. R.; Bach, S. B. H.; McElvany, S. W. *J. Chem. Phys.*, in press.

The Electronic Structure of K_2^{2-}

Francoise Tientega, James L. Dye,* and James F. Harrison*

Department of Chemistry, Michigan State University
East Lansing, Michigan 48824-1322

Received March 26, 1990

Revised Manuscript Received February 20, 1991

Recently the crystal structures of the alkalides $\text{K}^+(\text{C}_{222})\text{K}^-$ (I), $\text{Rb}^+(\text{C}_{222})\text{Rb}^-$ (II) and $\text{Rb}^+(\text{18C6})\text{Rb}^-$ (III) have been reported.¹ The alkali-metal anions form dimers in I and II and chains in III, in which the anion-anion distances are at least one angstrom shorter than expected from other alkalide structures. These results suggest that, in the crystal, a chemical bond exists between two K^- or Rb^- anions. We report here the results of ab initio electronic structure calculations on K_2^{2-} , which provide insight into a possible mechanism for the anion-anion bonding in these materials. The basis set used for K was constructed from Wachters'² 14s9p set by first contracting it to 8s5p and then adding the two p functions recommended by Wachters, followed by three diffuse s functions ($\alpha = 0.007649, 0.003542, 0.001640$), two diffuse p's ($\alpha = 0.005541, 0.002019$), and two diffuse d's ($\alpha = 0.09, 0.01$). The quality of the resulting (11s, 9p, 2d) basis was tested by calculating various properties of K, K_2^0 , and K_2^{1-} .

(1) Huang, R. H.; Ward, D. L.; Dye, J. L. *J. Am. Chem. Soc.* **1989**, *111*, 5707.

(2) Wachters, A. J. H. *J. Chem. Phys.* **1977**, *66*, 4245.

(13) The ^{13}C NMR spectra were obtained on a Varian UNITY 300 NMR spectrometer equipped with a variable-temperature broad-band switchable 5-mm probe. The ^7Li spectra were obtained on a Varian VXR-200 spectrometer equipped with a variable-temperature broad-band switchable 5-mm probe.

(14) According to ref 4k, C_{60} hexaanion should be more diamagnetic than neutral C_{60} . However, the paramagnetic contribution to the carbon chemical shift is greater in the hexaanion, resulting in net deshielding.

(15) The deshielding is 0.9 ppm/carbon.

(16) Hogen-Esch, T. E.; Smid, J. *J. Am. Chem. Soc.* **1967**, *89*, 2764.

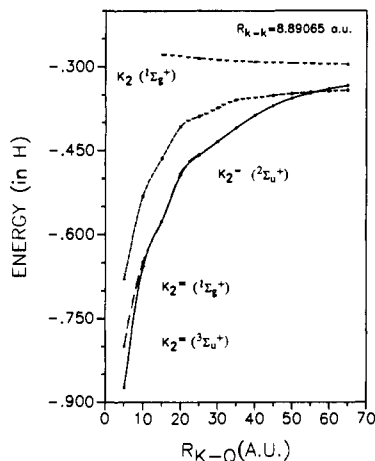
(17) At early stages of sonication (cloudy green-colored solution), no ^{13}C NMR signal could be detected. This solution was ESR active and showed a strong signal at the g value close to that of a free electron.

(18) Similarly, Vollhardt et al. found that quenching of the dianion of [3]phenylene with methanol gave an extremely air sensitive solid that upon exposure to even traces of air regenerated the starting [3]phenylene quantitatively. See: Berris, B. C.; Hovakeemian, G. H.; Lai, Y.-H.; Mestdagh, H.; Vollhardt, K. P. C. *J. Am. Chem. Soc.* **1985**, *107*, 5670.

Table I. Comparison of Calculated and Experimental Properties of K_2 and K_2^-

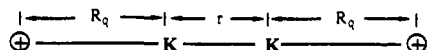
molecule	$R_e, \text{\AA}$		D_e, eV		ω_e, cm^{-1}	
	expt	theory	expt	theory	expt	theory
$K_2(^1\Sigma_g^+)$	3.904 ^a	4.152	0.520 ^a	0.493	92.0 ^a	84.0
$K_2^{1-}(^2\Sigma_u^+)$		4.678	0.512 ^b	0.500		56.7

^a Reference 4. ^b Value computed by using the available experimental data from the following: McHugh, K. M.; Eaton, J. G.; Lee, G. H.; Sarkas, H. W.; Kidder, L. H.; Snodgrass, J. T.; Manaa, M. R.; Bowen, K. H. *J. Chem. Phys.* **1989**, *91*, 3792.

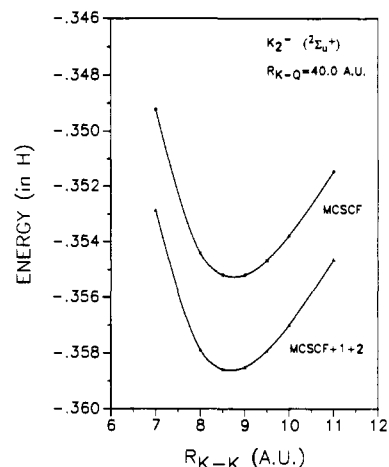
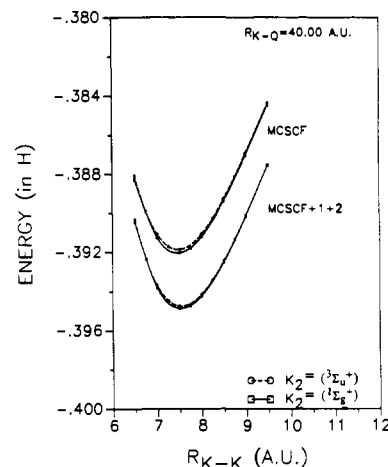
**Figure 1.** MCSCF energy (relative to -1198) of K_2^0 , K_2^{1-} , and K_2^{2-} as a function of the distance of point positive charges from either nucleus.

The electron affinity of K calculated with this basis at the CISD level is 0.494 eV (experimental³ value = 0.501 eV). Calculated properties for K_2^0 and K_2^{1-} are collected in Table I and compared with the available experimental data. These molecular calculations consist of all single and double excitations from a multiconfiguration reference space. The reference space for both K_2^0 and K_2^- was the CASSCF space formed from the 4s and 4p orbitals on each center.

Preliminary calculations on K_2^{2-} show that it is unbound relative to K_2^{1-} and a free electron. Since K_2^{2-} lies in the continuum of $K_2^{1-} + e$, conventional electronic structure calculations cannot reliably predict its structure. However, in the crystal where we suspect that a chemical bond exists between two K^{1-} anions, the ions are subject to various Coulombic interactions from the surrounding medium. Accordingly we augmented the free-molecule Hamiltonian with an electrostatic potential and field gradient generated by point charges placed along the internuclear axis as shown below:



In this environment there exists a R_{K-Q} for which K_2^{2-} is more stable than $K_2^{1-} + e$. Figure 1 shows the absolute energy of K_2 , K_2^{1-} , and K_2^{2-} ($^1\Sigma_g^+$ and $^3\Sigma_u^+$) as a function of R_Q . The K nuclei have been placed $\sim 4.5 \text{\AA}$ apart. The calculations use the MCSCF technique and include the CASSCF space formed from the 4s and 4p orbitals on each center. Note that the energy of K_2^0 is rather insensitive to the location of the charges and increases slightly as the charges approach the K nuclei. Presumably the repulsion is due to the positive quadrupole moment of K_2^0 interacting with the electric field gradient generated by the charges. When R_{K-Q} is < 55 au, both states of K_2^{2-} are bound relative to $K_2^{1-} + e$. Figure 2 shows the results of MCSCF and MCSCF+1+2 calculations on the $^2\Sigma_u^+$ state of K_2^{1-} when $R_{K-Q} = 40$ au. The bond length is 4.63 \AA , similar to the computed value of 4.68 \AA for free ($R_{K-Q} = \infty$) K_2^{1-} . Figure 3 shows the results of similar calculations on the $^1\Sigma_g^+$ and $^3\Sigma_u^+$ states of K_2^{2-} . These

**Figure 2.** MCSCF and MCSCF+1+2 energies (relative to -1198) of K_2^{1-} as a function of R when the point charges are 40 au from the K nuclei.**Figure 3.** MCSCF and MCSCF+1+2 energies (relative to -1198) of K_2^{2-} in the $^1\Sigma_g^+$ and $^3\Sigma_u^+$ states as a function of R when the point charges are 40 au from the K nuclei.**Table II.** Valence Natural Orbital Occupation at Equilibrium for K_2 , K_2^- , and K_2^{2-}

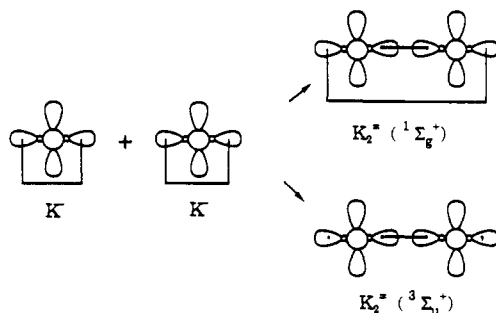
molecule	$6\sigma_g$	$6\sigma_u$	$7\sigma_g$	$7\sigma_u$
$K_2(^1\Sigma_g^+)$	1.76	0.13	0.03	0.0
$K_2^{2-}(^2\Sigma_u^+)$ free	1.74	0.97	0.14	0.01
$K_2^{1-}(^2\Sigma_u^+)$	1.74	0.97	0.14	0.01
$K_2^{2-}(^1\Sigma_g^+)$	1.79	0.86	1.14	0.08
$K_2^{2-}(^3\Sigma_u^+)$	1.79	1.00	1.00	0.08

two states are very close in energy and have essentially identical bond lengths ($R = 4.00 \text{\AA}$).

The occupancies of the dominant natural orbitals from the MCSCF calculation are shown for K_2^0 , K_2^{1-} , and K_2^{2-} in Table II. In the $^3\Sigma_u^+$ state the two extra electrons are in the $6\sigma_u$ and $7\sigma_g$ orbitals, which are essentially antibonding combinations of 4s and bonding combinations of 4p orbitals. Linear combinations of these orbitals localize the two electrons on each center in an sp hybrid directed away from the chemical bond. Since the $6\sigma_g^2 6\sigma_u^2$ and $6\sigma_g^2 7\sigma_g^2$ configurations have comparable weights in the MCSCF of the $^1\Sigma_g^+$, the NOs have the occupancies shown in Table II and a very similar electron distribution obtains for the both $^1\Sigma_g^+$ and $^3\Sigma_u^+$ states. In generalized valence bond⁴ terms we can imagine the bond in K_2^{2-} being formed between two correlated $^1S, K^{1-}$ ions by uncoupling the singlet-coupled electron pair on both ions and then singlet coupling two of these electrons

(3) Hotop, H.; Lineberger, W. C. *J. Phys. Chem. Ref. Data* **1975**, *A*, 539.(4) Goddard, W. A., III; Dunning, T. H., Jr.; Hunt, W. J.; Hay, P. J. *Acc. Chem. Res.* **1973**, *6*, 368.

into a σ bond and leaving the remaining two electrons localized on very different orbitals on each K ion.



The observed K^- to K^- distance in I is 4.90 Å, considerably longer than the 4.00 Å that we calculate. This suggests that the particular electrostatic potential we have used overestimates the positive potential experienced by K_2^{2+} . While we are exploring⁵ more realistic potentials based on the observed crystal structure, we feel that these calculations suggest that a reasonable mechanism for the anion-anion bonding in alkalides is the stabilization of K_2^{2-} by the internal electric fields in the crystal.

Acknowledgment. This research was supported, in part, by NSF Grants CHE 85-19752 (J.F.H.) and DMR 87-14751 (J.L.D.).

(5) Tientega, F.; Dye, J. L.; Harrison, J. F. The Electronic Structure of Na_2^{2-} and K_2^{2-} , in preparation.

Systematic Sensitivity Analyses in Free Energy Perturbation Calculations

Chung F. Wong

Mount Sinai School of Medicine
 Department of Physiology and Biophysics
 New York, New York 10029-6574
 Received October 22, 1990

The use of free energy perturbation calculations is increasing gradually in chemistry and biochemistry.¹ Since the potential energy functions used in these calculations are approximate, it is important to examine the sensitivity of simulation results to the choice of the parameters in these potentials. The response of a free energy result ($\Delta A = A_2 - A_1$: the free energy difference between state 2 and state 1) to a small change in a potential parameter can be obtained by recalculating ΔA with two or more values of the parameter. However, this would be an expensive procedure by which to examine the response of ΔA to each parameter in the potential energy function. An alternative based on the systematic sensitivity analysis method² (SSAM) commonly used in engineering problems is proposed here for the analyses of free energy results. The advantage of the method is that it requires only two simulations to find out the sensitivity of ΔA to a small change in each parameter in the potential energy function.

Using the sensitivity analysis approach,² one approximates the response ($\Delta\Delta A$) of ΔA to parameter changes by a truncated Taylor series:

$$\Delta\Delta A = \sum(\delta\Delta A/\delta\lambda_i)\Delta\lambda_i \quad (1a)$$

$$= \sum(\delta A_2/\delta\lambda_i)\Delta\lambda_i - \sum(\delta A_1/\delta\lambda_i)\Delta\lambda_i \quad (1b)$$

where $\Delta\lambda_i$ represents a small change in the parameter λ_i . The

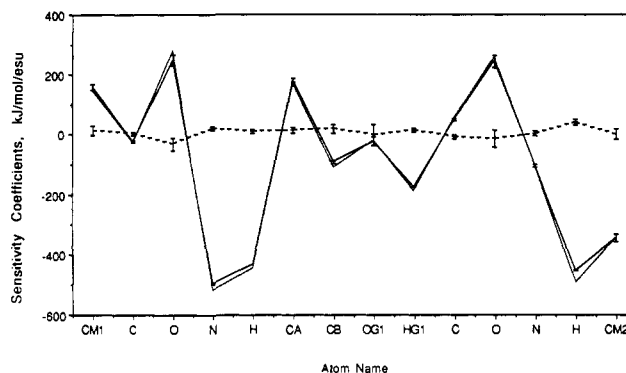


Figure 1. $\delta A_2/\delta\lambda_i$ (dotted line), $\delta A_1/\delta\lambda_i$ (solid line), and $\delta\Delta A/\delta\lambda_i$ (dashed line); see text for description. The molecular dynamics simulation of the threonine "dipeptide" was performed with the GROMOS⁴ molecular modeling package using a time step of 2 fs. The SHAKE algorithm⁵ was used to constrain the covalent bond lengths. Periodic boundary conditions were used in the simulation. The threonine "dipeptide" was put in a box of 230 equilibrated methanol molecules. After 25ps of careful equilibration, the sensitivity coefficients were calculated using data from the next 30ps (i.e. 25-55ps). Each error bar was estimated from the difference of corresponding sensitivity coefficients calculated from two 15ps segments. At 55ps, the threonine "dipeptide" was "mutated" into a serine "dipeptide". The system was allowed to relax for 10ps and sensitivity coefficients were calculated from data of the next 30ps. For clarity, error bars of $\delta A_2/\delta\lambda_i$ are not shown. The error bar of each $\delta\Delta A/\delta\lambda_i$ is obtained by adding the error bars of $\delta A_2/\delta\lambda_i$ and $\delta A_1/\delta\lambda_i$. The OPLS⁶ parameters were used for the methanol molecules. The GROMOS⁴ parameters were used for the "dipeptides". The combination rules described in reference 4 were used to construct the interaction potential between the "dipeptides" and the methanol molecules.

partial derivatives $\delta\Delta A/\delta\lambda_i$'s, which are known as sensitivity coefficients, can be calculated by using the finite difference formula:

$$\delta\Delta A/\delta\lambda_i = -[1/(2\beta d\lambda_i)] \times \{ \ln \{ \langle \exp[-\beta(H_2(\lambda_i + d\lambda_i) - H_2(\lambda_i))] \rangle_{2/\lambda_i} / \langle \exp[-\beta(H_2(\lambda_i - d\lambda_i) - H_2(\lambda_i))] \rangle_{2/\lambda_i} \} - \ln \{ \langle \exp[-\beta(H_1(\lambda_i + d\lambda_i) - H_1(\lambda_i))] \rangle_{1/\lambda_i} / \langle \exp[-\beta(H_1(\lambda_i - d\lambda_i) - H_1(\lambda_i))] \rangle_{1/\lambda_i} \} \} \quad (2)$$

where $\beta = (\text{Boltzmann constant} \times \text{absolute temperature})^{-1}$, $H_i(x)$ is the classical Hamiltonian of the state i evaluated by using the potential parameter x , and $\langle \dots \rangle_{j/\lambda_i}$ represents an ensemble average over the state j simulated by using the potential parameter λ_i . $d\lambda_i$ is a small finite change in the parameter λ_i . Similar finite difference formulas have been used to calculate enthalpy and entropy changes.³

The SSAM was tested by taking ΔA to be the free energy difference between *N*-acetylserine *N*-methylamide (state 2) and *N*-acetylthreonine *N*-methylamide (state 1) in methanol. Results for $\delta A_2/\delta\lambda_i$, $\delta A_1/\delta\lambda_i$, and $\delta\Delta A/\delta\lambda_i$ in which λ_i 's are the atomic partial charges of the "dipeptides" are shown in Figure 1. Since corresponding atoms in the two "dipeptides" have similar free energy responses to small changes in the atomic partial charges (i.e., $\delta A_2/\delta\lambda_i \approx \delta A_1/\delta\lambda_i$), $\delta\Delta A/\delta\lambda_i$'s have values close to 0. Equation 1a then suggests that ΔA is not sensitive to small parameter changes. To quantify this further, it is useful to take each $\Delta\lambda_i$ as $\Delta\lambda_i = \lambda_i(V_a) - \lambda_i(V_b)$ where $\lambda_i(V_a)$ and $\lambda_i(V_b)$ are the atomic partial charges from force fields V_a and V_b , respectively (V_b is the force field used in the simulation; see figure caption). One can then estimate $\sum(\delta A_2/\delta\lambda_i)\Delta\lambda_i$, $\sum(\delta A_1/\delta\lambda_i)\Delta\lambda_i$, and $\Delta\Delta A$ in eq 1b. When V_a is taken to be the AMBER⁷ force field, \sum -

(3) Fleischman, S. H.; Brooks, C. L., III. *J. Chem. Phys.* **1987**, *87*, 3029.

(4) van Gunsteren, W. F. *GROMOS*; University of Groningen: Groningen, 1987. Hermans, J.; Berendsen, H. J. C.; van Gunsteren, W.; Postma, J. P. M. *Biopolymers* **1984**, *23*, 1513.

(5) Ryckaert, J. P.; Ciccoliti, G.; Berendsen, H. J. C. *J. Comput. Phys.* **1977**, *23*, 327.

(6) Jorgensen, W. L. *J. Phys. Chem.* **1986**, *90*, 1276. Jorgensen, W. L. *J. Am. Chem. Soc.* **1984**, *106*, 6638.

(7) Weiner, S. J.; Kollman, P. A.; Case, D. A.; Singh, U. C.; Ghio, C.; Alagona, G.; Profeta, S.; Weiner, P. *J. Am. Chem. Soc.* **1984**, *106*, 765.